Sabancı University

MAT 306 - Computational Techniques for Materials at the Nano-scale

Conformational Map of Cyclohexane

Homework 1 - Report

Submitted by:

Kadir Yağız EBİL

March 20, 2025

Contents

1 Aim

The aim of this study is to construct the conformational surface of cyclohexane (C_6H_{12}) using molecular dynamics (MD) simulations. By analyzing the dihedral angle changes over time, we aim to understand the energy landscape and stability of different states of the molecule, heat barier height, prefered states and many morex.

2 Introduction

Cyclohexane is one of the most important structures in chemistry, exhibiting multiple stable conformations due to its ring structure. Understanding its conformational map is essential for applications in material science and many more. In this report, we will perform MD simulations at high temperatures (1000K) to sample different conformations and construct a gibbs free-energy(?) surface and understand behaviour of cyclohexane.

3 Methods

3.1 Simulation Setup

The simulation was performed using the molecular dynamics software, NAMD[3], with the following parameters:

- Initial structure (chair conformation): Provided as `cyclohexane.psf` and `cyclohexane.pdb` files.

- Temperature: 1000 K.

- Simulation time: 10 nanosecond (10,000 frame).

- Time step: 1 fs.

- Force field: CHARMM.

- Periodic boundary conditions: Enabled.

- Thermostat: Langevin thermostat with damping coefficient of 10.

3.2 Simultaion Run

Simulation run by following command:

```
namd2 +p6 cyclohexane.namd > 1000k_run.txt
```

3.3 Data Analysis

The simulation output was analyzed to extract:

- Actualy tempreture of the system and variations.

- Trajectories of dihedrals.

- Density and sampling plots of dihedrals (2D and 3D).

- Dihedral matrix.

- PMF of dihedrals (2D and 3D).

- Probability comparison for dihedral angles.

- Global extrema and local extrema for dihedral angles.

- Energy differences between minima and barrier heights.

- Trajectory of distance between two sides of molecule.

- Cremer Pople distributions and trajectories of molecule.

3.4 AI Assistance

- Coding: AI tools were used for script debugging; chatgpt, claude.ai, copilot.

- Summarization: AI tools assisted in refining the textual content of the report, finding referances; only chatgpt.

4 Results

4.1 Temperature Analysis

To verify the stability of the simulation, the temperature fluctuations were analyzed over time. The system was expected to maintain an average temperature of 1000 K with some natural variations due to the unpredictable nature of molecule dynamics.
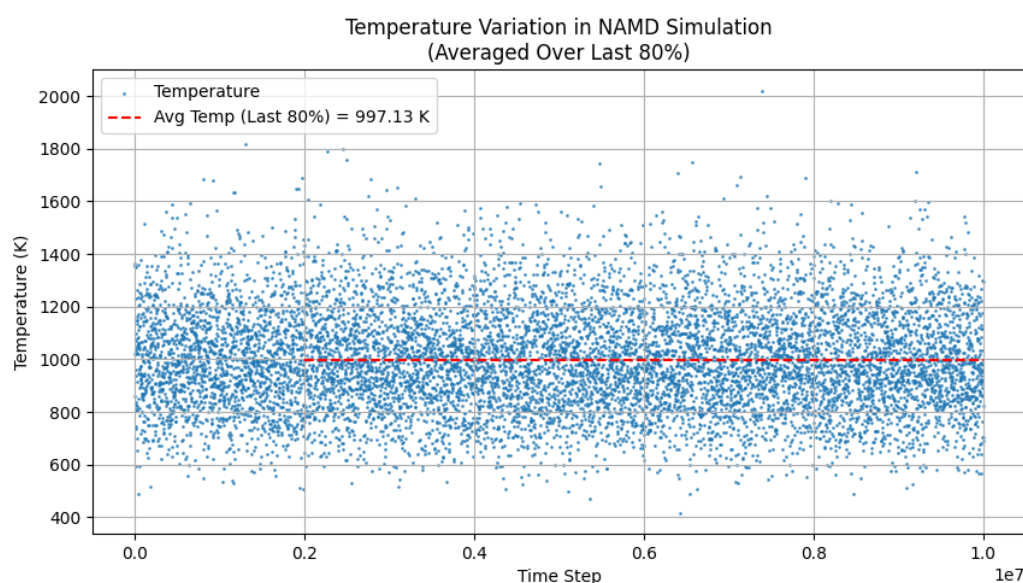

Figure 1: Temperature variations over the simulation time.

The results indicate that the temperature remained close to the target value with minimal fluctuations, ensuring a stable simulation environment.

4.1.1   Temperature Analysis without Langevin Thermostat

Before Langevin Thermostat was initialized inside namd parameter file, to achieve 1000K average, inital temperature was set to 1500K expecting average of 1000K. As an interesting result, we observed hyperbolic temperature samples 2 at the end of the simulation. Reason is still unknown.
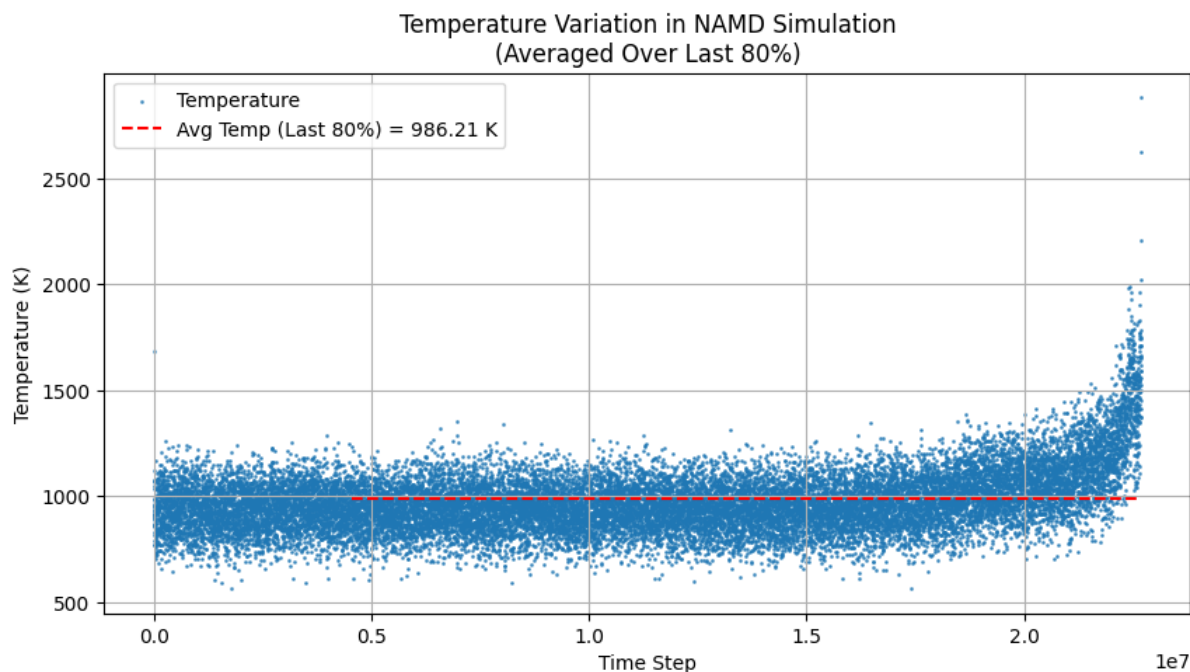

Figure 2: Temperature variations without Langevin Thermostat.

4.2   Dihedral Trajectories

The dihedral angles were extracted from the simulation trajectory, and their time evolution was analyzed. This allowed us to identify the transitions between different conformational states and relationship of internal dihedrals.
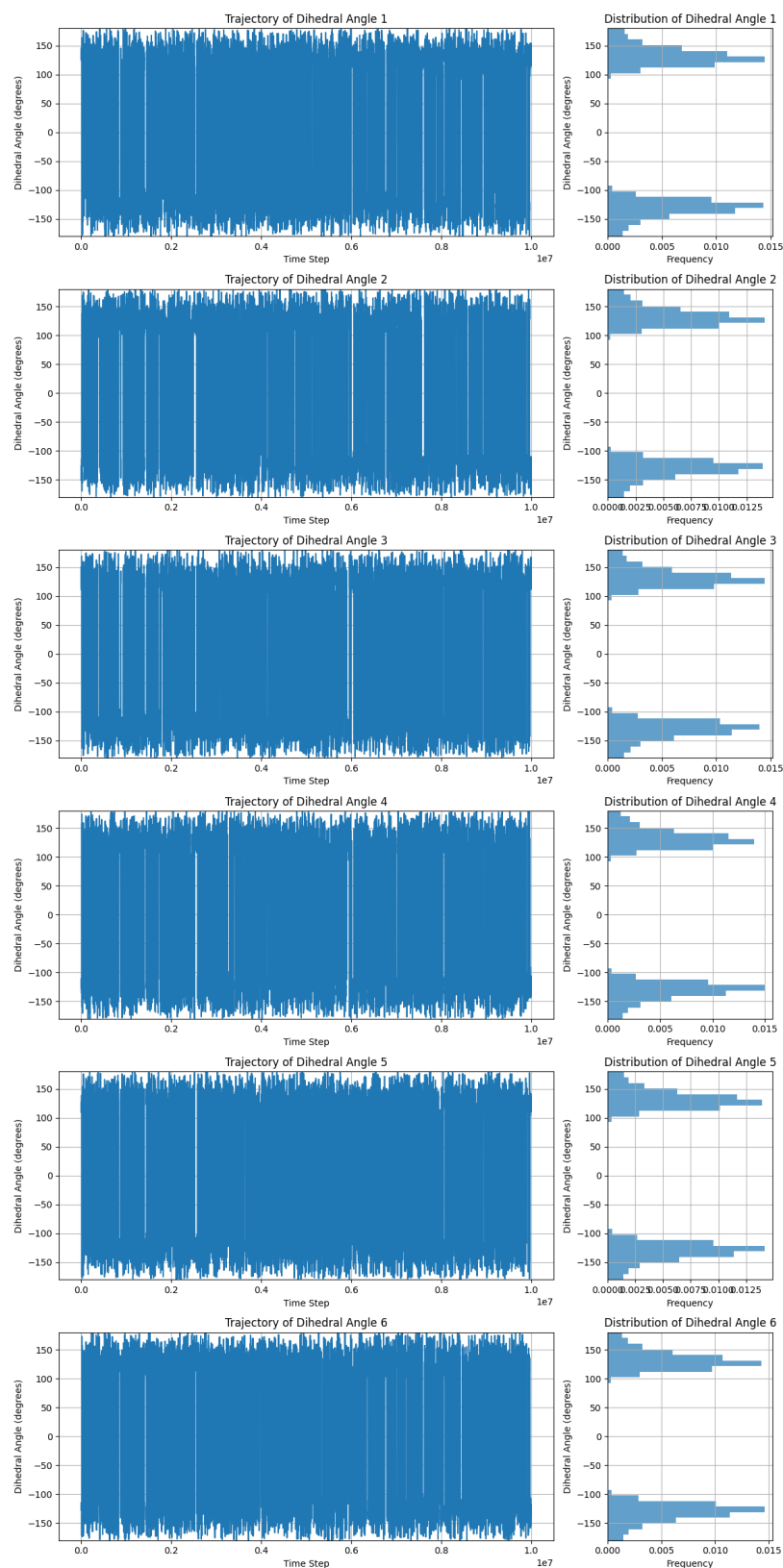
Figure 3: Dihedral angle trajectories over time.

From Figure 3, we observe multiple conformational changes, indicating that the system has sampled various states many times, including chair, boat, and twist-boat conformations.

4.3   Dihedral Probability Distributions

To quantify the likelihood of different conformational states, the probability distribution of dihedral angles was computed. As shown in Figure 3, dihedrals angles tend to stay at the regions of, 100 to 180 and -180 to -100. Exact probabilities calculates and presented in Table 1.

Dihedral Angle	Region 1	Region 2	Region 3
Dihedral Angle 1	0.493	0.000	0.507
Dihedral Angle 2	0.500	0.000	0.500
Dihedral Angle 3	0.503	0.000	0.497
Dihedral Angle 4	0.500	0.000	0.500
Dihedral Angle 5	0.495	0.000	0.505
Dihedral Angle 6	0.509	0.000	0.491

Table 1: Probability distribution of dihedral angles across different regions.

The peaks in Figure 3 correspond to the most frequently visited conformations. These results provide insight into the preferred conformational states of cyclohexane which is known as chair conformation[5].

4.4   Sampling and Density

Dihedrals density plots indicate that certain dihedral angle pairs are favored, which corresponds to chair conformations, while lower-density regions represent higher-energy states such as the boat or twist-boat conformations[5]. Altough transitions between the clusters suggest occasional shifts between conformers, which occur due to thermal fluctuations.

4.4.1   Dihedral relations

We also observed in Figure 5 that Dihedral angles 1 and 2 tend to change together, because they are closer in the ring structure. Dihedral angles 1 and 4 are further apart, leading to weaker direct correlation and more possible conformations as seen in Figure 6. We didn't have enough time to fully explain the reason of very little change in Figure 4 but probably because of the placement of dihedral angles 3 and 6 is exactly opposite[6].
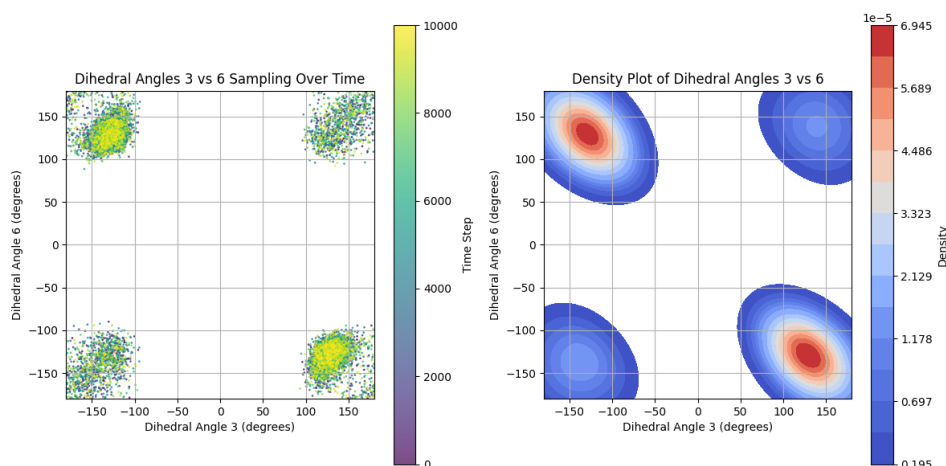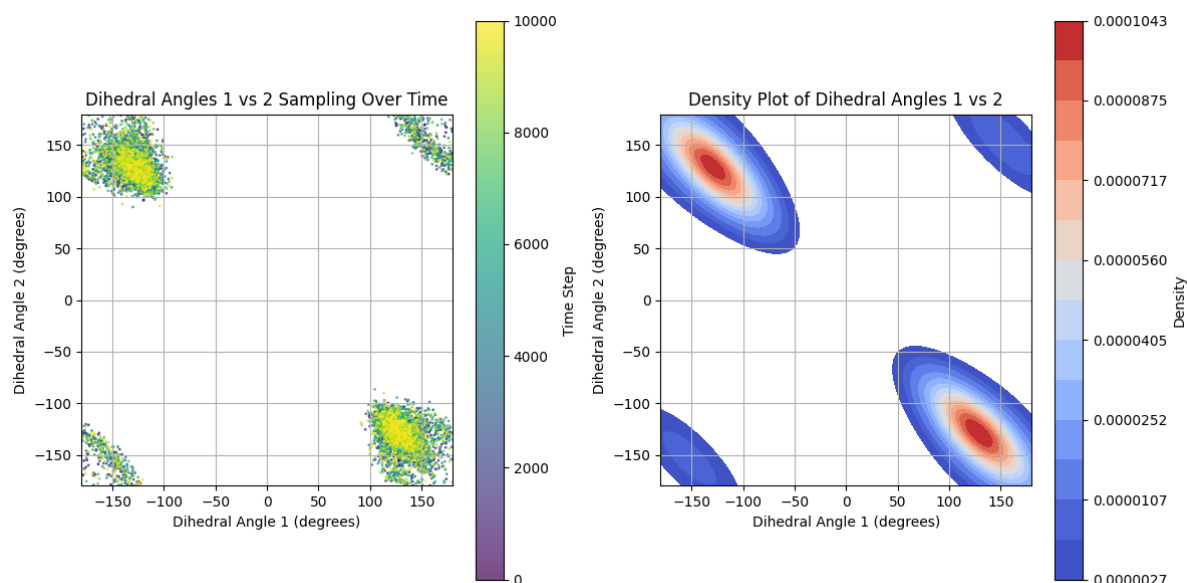

Figure 4: 2D representation of dihedrals 3 and 6.
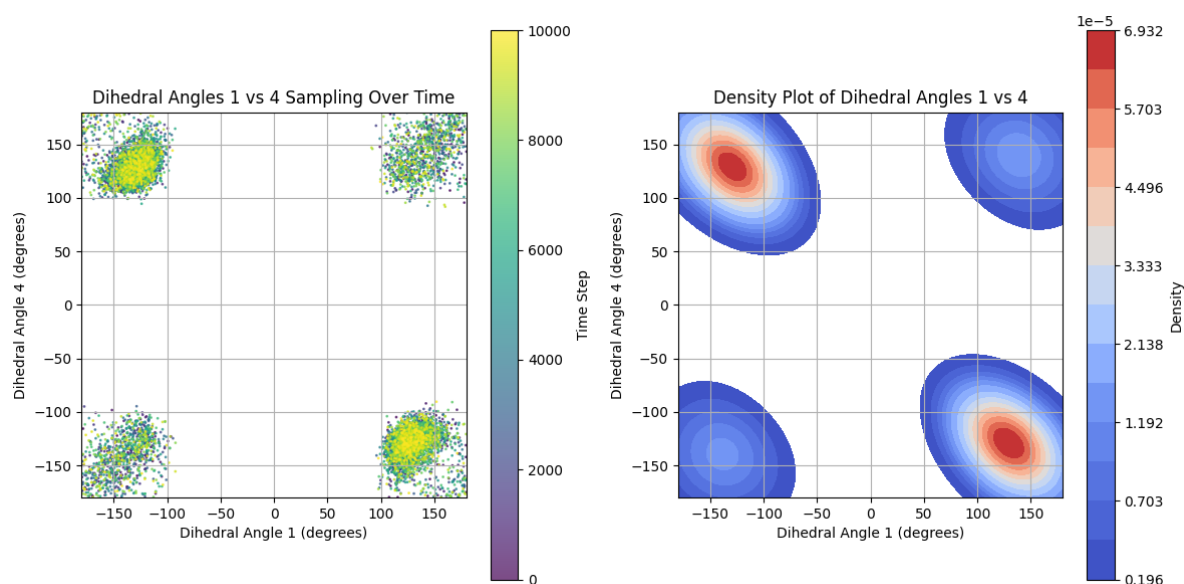
6

Figure 5: 2D representation of dihedrals 1 and 2.

Figure 6: 2D representation of dihedrals 1 and 4.

4.4.2   3D and Matrix Versions of Density Plots

To be able to observe all possibble correlations between dihedrals we reshaped our data into matrix format..The correlation matrix in Figure 7 shows strong dependencies between certain dihedral angles, reflecting the cooperative motion of the ring structure.
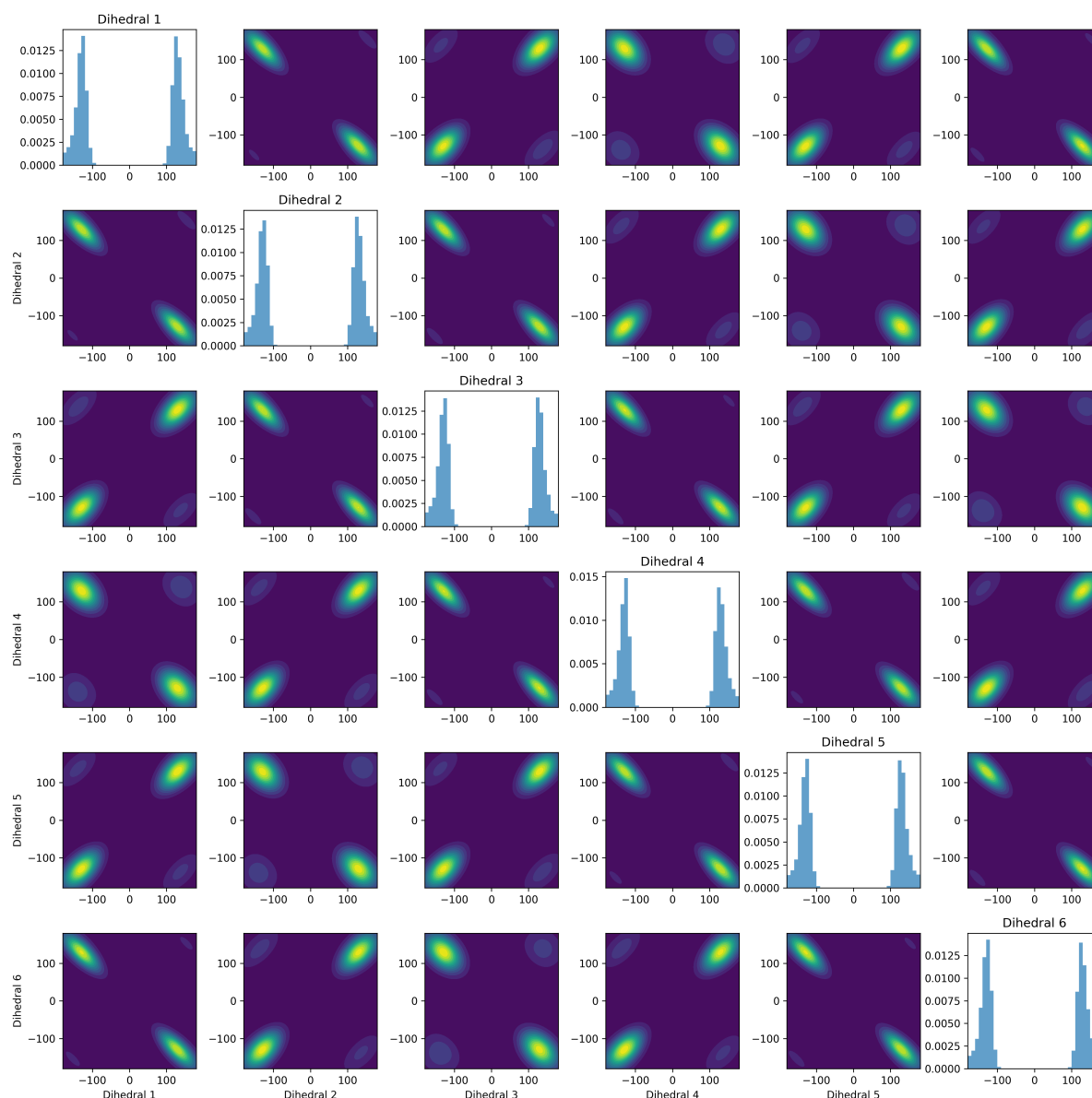
7

Figure 7: Dihedral angle correlation matrix.

Compared to the 2D contour plot, the height of the peaks helps quantify the significance of different conformational states. The 3D surface makes it easier to see the gradual changes in density. Again there are visible differences between Figure 8 and Figure 9 due to placement of dihedreals inside the ring.
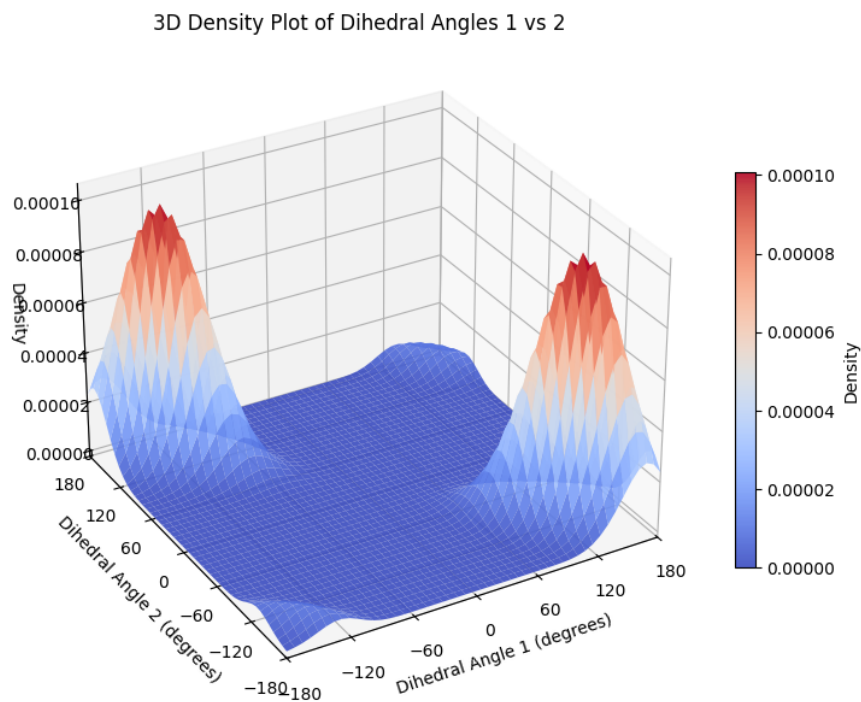
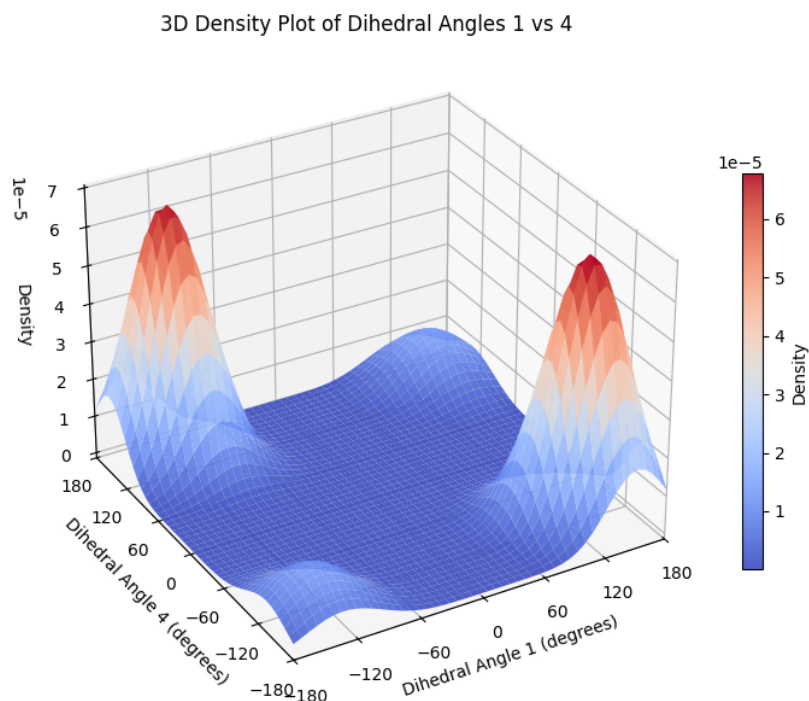Figure 8: 3D representation of dihedrals 1 and 2.

Figure 9: 3D representation of dihedrals 1 and 4.

4.5   Conformational Energies and PMF's

The energy differences between different conformations were calculated, as shown in Table 2. These values are also checked agins literature, also there is a noise literature seems

to fit our data[1].

Conformation Pair	Energy Difference (kJ/mol)	Barrier Height (kJ/mol)
Chair $\leftrightarrow$ Boat	29.3572	45.9345
Chair $\leftrightarrow$ Twist-Boat	23.4262	41.5027
Boat $\leftrightarrow$ Twist-Boat	5.5530	8.2372

Table 2: Energy differences and barrier heights between cyclohexane conformations.

These values provide insight into the thermodynamic and kinetic stability of each conformation. Barriers and maximum and minimum energy, spots observed. Energy potential energy storage capability in Figure 10 much less significant compared to Figure 11 due to placement of this dihedrals.
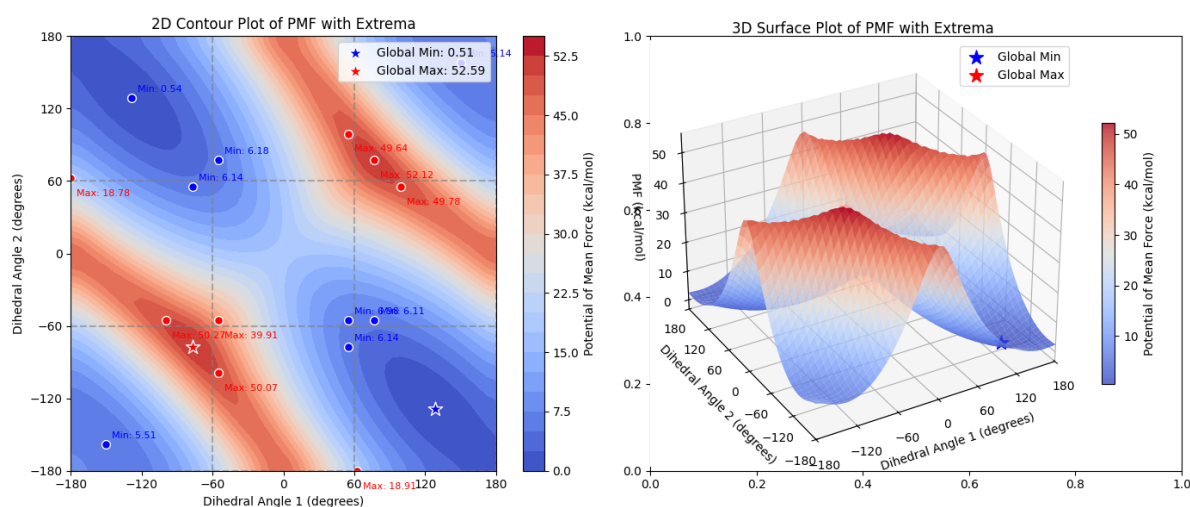

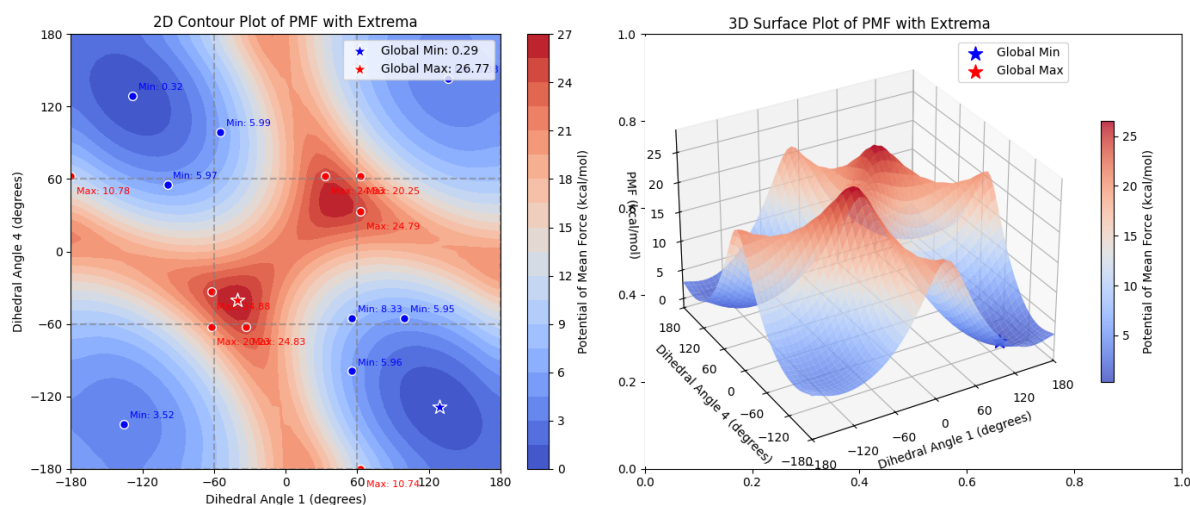Figure 10: PMF of cyclohexane conformations dihedrals 1 and 2.

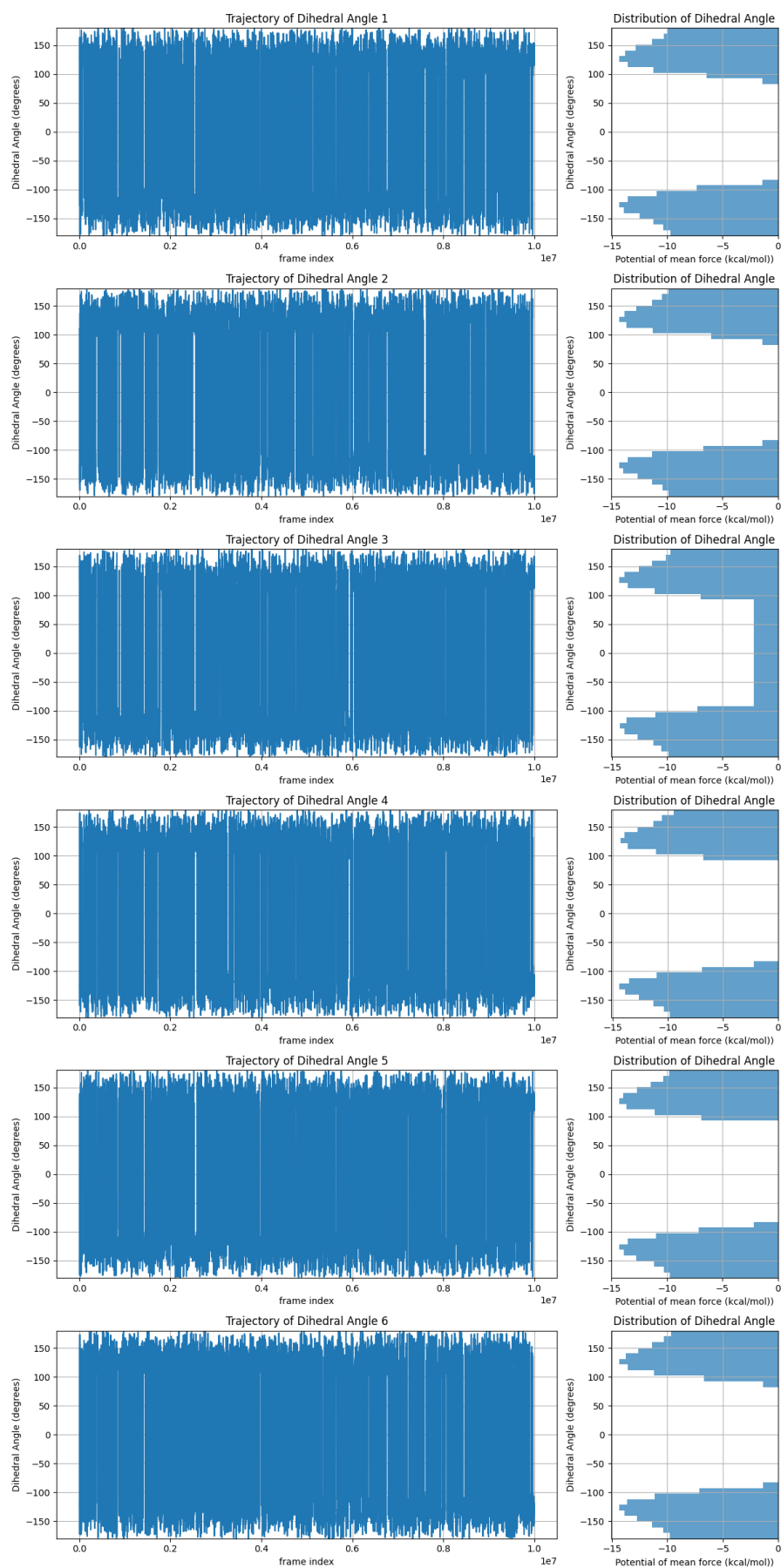Figure 11: PMF of cyclohexane conformations dihedrals 1 and 4.

Figure 12: Potential of mean force PMF of cyclohexane conformations.

4.6   Trajectory of Molecular Distance

The distance between two reference points on the molecule (Carbons numbered as 0 and 3) was tracked to monitor structural deformations. While in chair conformation distance is around 3 angstrom, while in boat conformation the opposing carbons get closed to each other almost 1 angstrom. The trajectory analysis of this distance in Figure 13 shows the changes happend to cyclohexane.
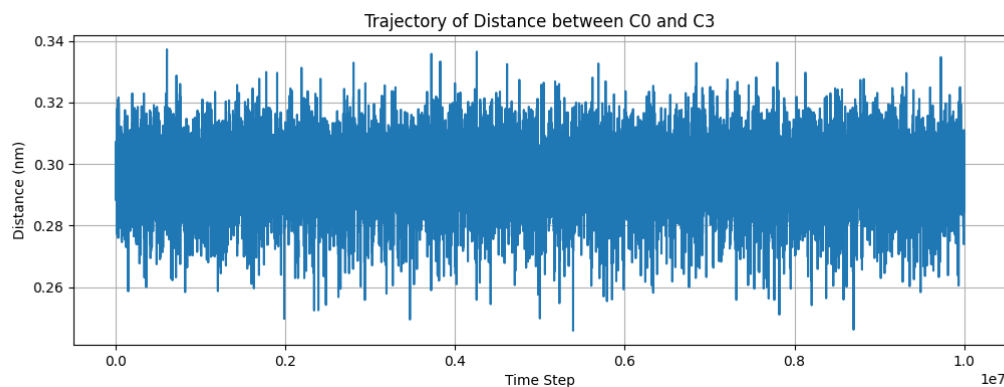

Figure 13: Trajectory of the distance between two sides of the molecule.

This analysis helps confirm structural changes corresponding to transitions between different conformations.

4.7   Cremer-Pople Analysis

The conformational behavior of cyclohexane was analyzed using the Cremer-Pople parameters[7], which provide a quantitative framework for describing the puckering motion of six-membered rings. These parameters allow for a systematic representation of the flexibility and dynamic behavior of the ring, which is particularly important in the context of molecular simulations [2].

The Cremer-Pople formula(system) expresses the distortions of a six-membered ring in terms of;

- Puckering amplitude Q

- Puckering angle θ

- Puckering phase ϕ

These parameters are derived from the atomic displacements in the normal mode coordinate(simple plane structure) system of the ring[7].

4.7.1   Mathematical Definition of Cremer-Pople Parameters

For a six-membered ring with atomic positions denoted by Cartesian coordinates (x_i, y_i, z_i), the puckering coordinates q_i are computed by projecting the displacements on to the normal modes of the ring. These coordinates are given by:

$$Q = \sqrt{\sum_{i=1}^{6} q_i^2} \tag{1}$$

where q_i represents the atomic puckering displacement for each of the six atoms.
The puckering angle θ is defined as:

$$\theta = \tan^{-1} \left(\frac{\sqrt{q_2^2 + q_3^2}}{q_1} \right) \tag{2}$$

where q_1, q_2, and q_3 correspond to different normal mode contributions that define the extent of puckering.

The puckering phase angle ϕ is given by:

$$\phi = \tan^{-1} \left(\frac{q_3}{q_2} \right) \tag{3}$$

which describes the specific conformation within the puckered states.

These three parameters together allow us to express the out-of-plane distortion in spherical coordinates Figure 14, making it easier to differentiate between the chair, boat, and twist-boat conformations and observe their frequency.
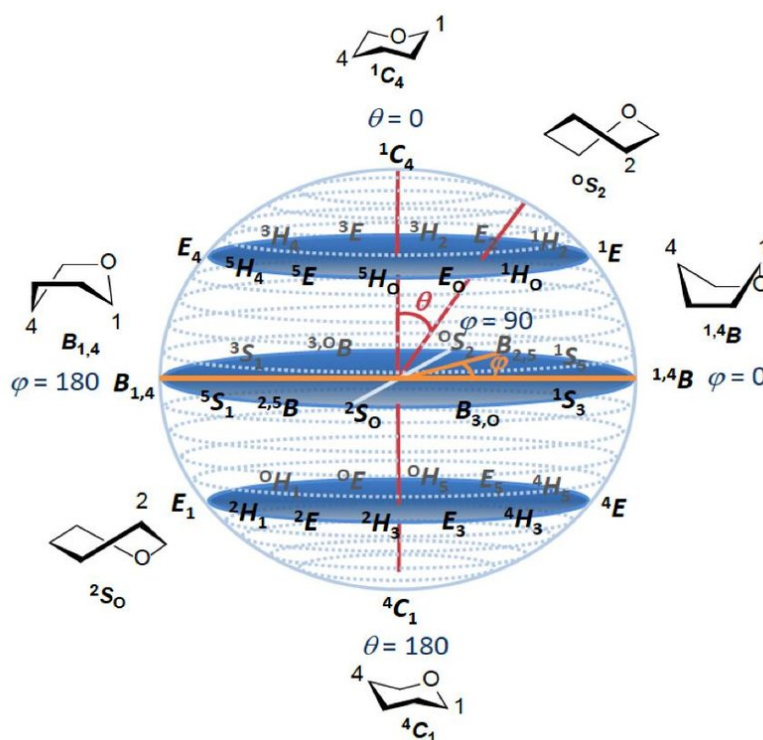

Figure 14: Spherical Coordinates [4].

4.7.2   Energy Landscape and Conformational Distribution

To better understand the conformational preferences of cyclohexane, we plot the distribution of Cremer-Pople parameters obtained from molecular simulations.
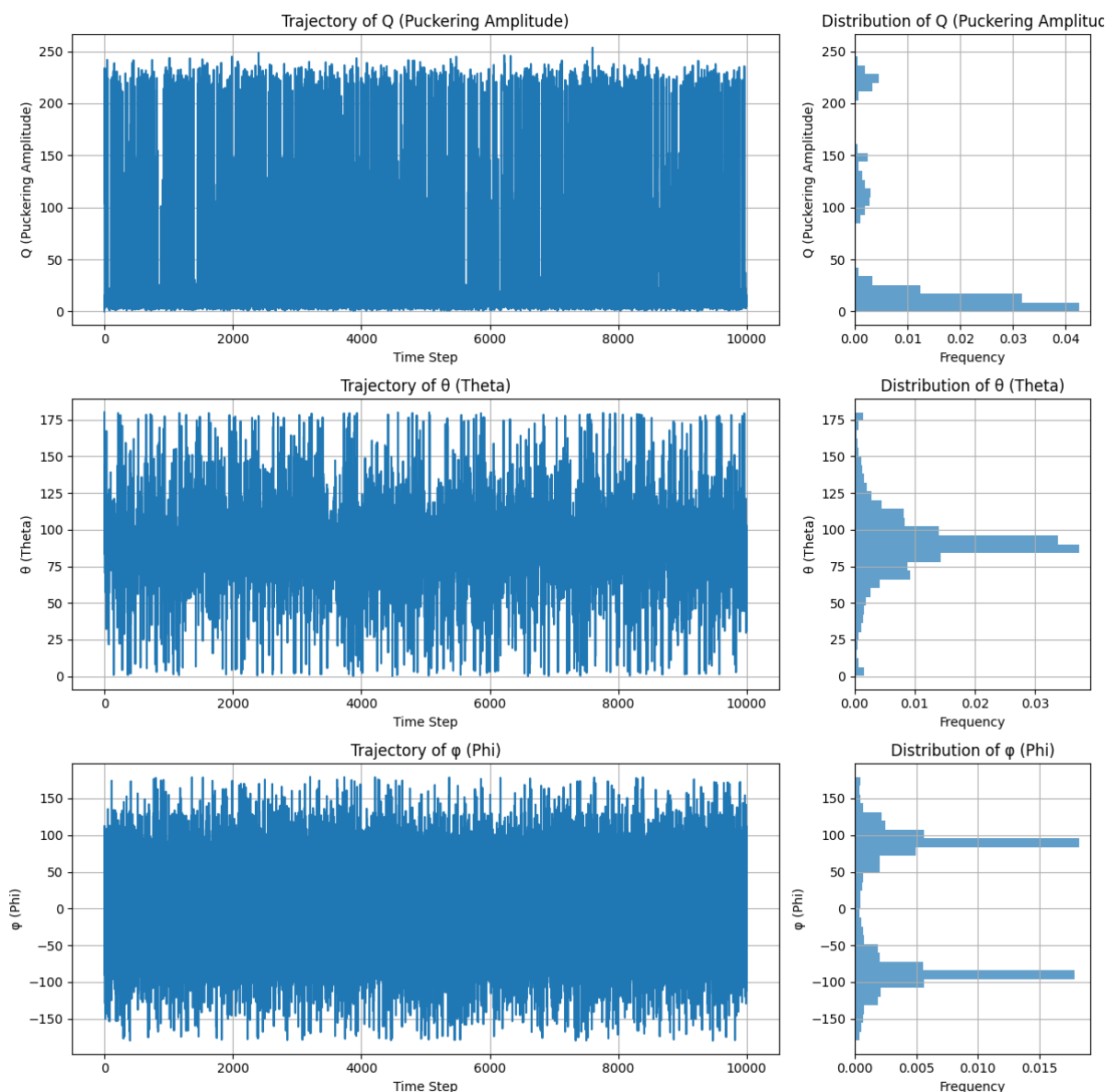
13

Figure 15: Time-dependent trajectory and histogram of Cremer-Pople parameters (Q, θ, ϕ) in cyclohexane. The left panel shows the evolution of the parameters over simulation time, while the right panel presents their probability distributions.

The results in Figure 15 demonstrate the distribution of conformations in Cremer-Pople space, providing insight into the naturally dominant ring-puckering state(s). The most frequently observed values correspond to stable conformation is the chair form, which shows itself as Q = 0, while transitions to higher energy boat-like conformations appear as fluctuations.

4.7.3 Energy Landscape Analysis in Cremer-Pople Space

To further investigate the energy landscape, we map the energy of different puckered conformations as a function of Q and θ, as shown in Figure 16.

This energy map in Figure 16 highlights the following:

- Low-energy regions (dark colors) correspond to stable conformations, primarily the chair form.

- High-energy regions (bright colors) correspond to less stable or transition-state conformations such as the boat and twist-boat.

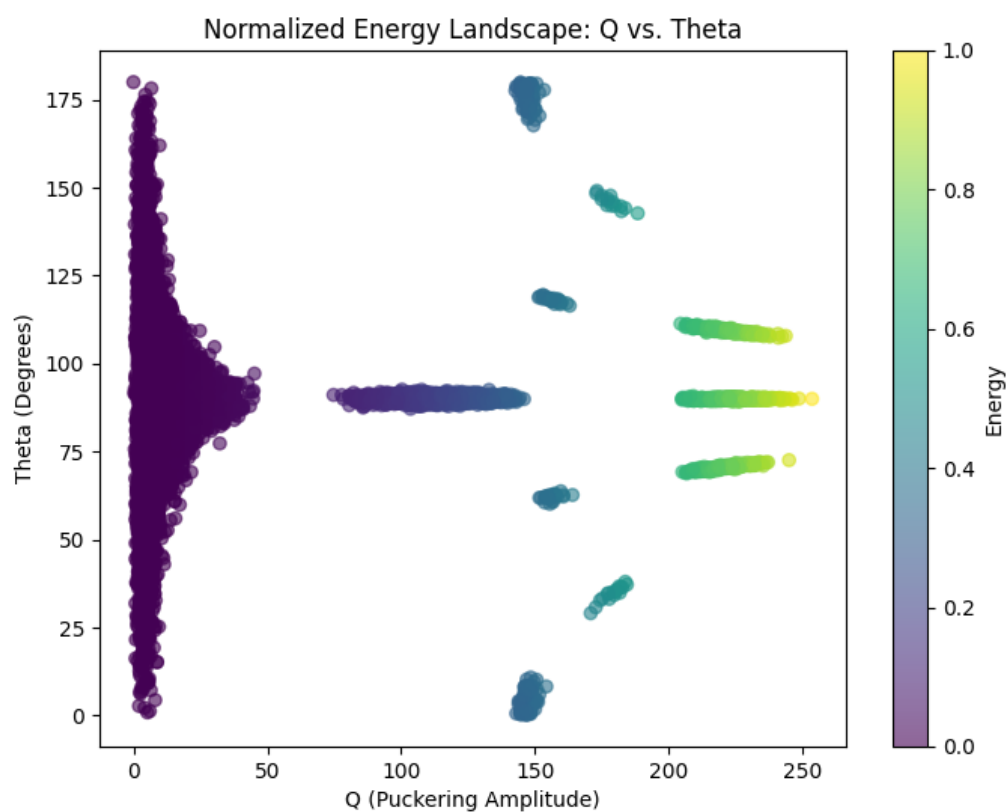- The spread of data points represents thermal fluctuations between conformational states.

Figure 16: Energy landscape of cyclohexane as a function of Cremer-Pople parameters Q (puckering amplitude) and θ (puckering angle). The color scale represents normalized energy.

A 3D visualization of this energy distribution in Figure 17 provides a more comprehensive view of the energy topology by showing the energy differences in terms of normalized values.
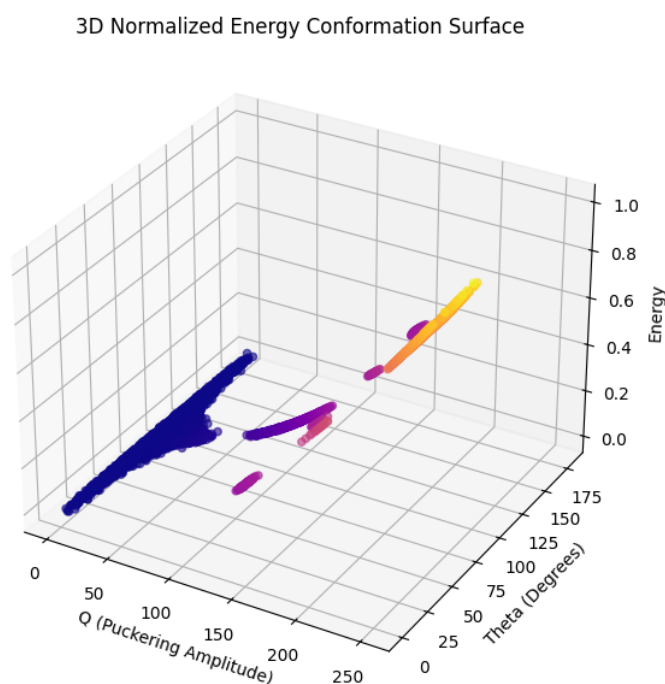
Figure 17: Three-dimensional energy conformation surface based on Q (puckering amplitude) and θ (puckering angle). The color gradient represents energy levels.

5   Conclusions

The MD simulations provided insight into the conformational preferences of cyclohexane. The choice of high temperature (1000 K), also a little experiment with (1500K), and facilitated efficient sampling of different states, allowing for a well-resolved conformational map.

To improve the accuracy of the results:

- Longer simulations could be conducted to enhance statistics.

- Lower temperatures could be explored to determine equilibrium conformational distributions.

- Better and better visualization techniques could be used.

References

[1] Steven Farmer et al. *4.5: Conformations of Cyclohexane*. URL: https://chem.libretexts.org/Bookshelves/Organic_Chemistry/Organic_Chemistry_%28Morsch_et_al.%29/04%3A_Organic_Compounds_-_Cycloalkanes_and_their_Stereochemistry/4.05%3A_Conformations_of_Cyclohexane.

[2] "Front Matter". In: *Nomenclature of Organic Chemistry*. The Royal Society of Chemistry, Dec. 2013. ISBN: 978-0-85404-182-4. DOI: 10.1039/9781849733069-FP001. URL: https://doi.org/10.1039/9781849733069-FP001.

[3] William Humphrey, Andrew Dalke, and Klaus Schulten. "VMD – Visual Molecular Dynamics". In: *Journal of Molecular Graphics* 14 (1996), pp. 33–38.

[4] Shiho Minakata et al. "Protein C-Mannosylation and C-Mannosyl Tryptophan in Chemical Biology and Medicine". In: *Molecules* 26 (Aug. 2021), p. 5258. DOI: 10.3390/molecules26175258.

[5] Wikipedia contributors. *Cyclohexane conformation — Wikipedia, The Free Encyclopedia*. [Online; accessed 20-March-2025]. 2025. URL: https://en.wikipedia.org/w/index.php?title=Cyclohexane_conformation&oldid=1280579224.

[6] Wikipedia contributors. *Ring flip — Wikipedia, The Free Encyclopedia*. [Online; accessed 20-March-2025]. 2025. URL: https://en.wikipedia.org/w/index.php?title=Ring_flip&oldid=1280568054.

[7] Wenli Zou, Yunwen Tao, and Elfi Kraka. "Systematic description of molecular deformations with Cremer–Pople puckering and deformation coordinates utilizing analytic derivatives: Applied to cycloheptane, cyclooctane, and cyclo[18]carbon". In: *The Journal of Chemical Physics* 152.15 (Apr. 2020), p. 154107. ISSN: 0021-9606. DOI: 10.1063/1.5144278. eprint: https://pubs.aip.org/aip/jcp/article-pdf/doi/10.1063/1.5144278/13396081/154107_1_online.pdf. URL: https://doi.org/10.1063/1.5144278.